Journal of Fluorine Chemistry 131 (2010) 1356–1361

Contents lists available at ScienceDirect

Journal of Fluorine Chemistry

journal homepage: www.elsevier.com/locate/fluor

Fluorinated modification of hyperbranched polyesters used for improving the surface property of UV curing coatings

Hui Miao, Fenfen Bao, Liangliang Cheng, Wenfang Shi [*]

CAS Key Laboratory of Soft Matter Chemistry, Department of Polymer Science and Engineering, University of Science and Technology of China, Jinzhai Road 96, Hefei, Anhui 230026, PR China

ARTICLE INFO

Article history:
Received 17 May 2010
Received in revised form 26 September 2010
Accepted 27 September 2010
Available online 29 October 2010

Keywords:
Hyperbranched polyester
Fluorinated
UV curing
Water and oil repellency
Coating

ABSTRACT

The commercial hyperbranched aliphatic polyols (H*n*) were modified by thioglycolic acid (TA) and hexafluorobutyl acrylate (HFBA) or dodecafluoroheptyl methacrylate (DFHMA) to prepare a series of fluorinated hyperbranched polyesters. For comparison, a linear fluorinated polymer, poly(*n*-BMA-co-DFHMA), was synthesized through the copolymerization of *n*-butyl methacrylate (BMA) and DFHMA. The molecular structures were characterized by ^{1}H NMR spectroscopic analysis. The synthesized polymers were incorporated into UV-curable formulations as additives, and exposed to a UV lamp. After UV curing, the wettability of the films was investigated by contact angle measurement with water and 1-bromonaphthalene. The results showed that both the hydrophobicity and oleophobicity were greatly enhanced. Moreover, the fluorinated hyperbranched polymers possessed better water and oil repellency than the copolymer poly(*n*-BMA-co-DFHMA) at a very low concentration. The surface F/C ratio values of the cured films were detected by XPS analysis, and the film with TAH20–DFHMA showed the highest F/C ratio value, indicating its most efficient aggregation effect at the film surface.

1. Introduction

Over past two decades, hyperbranched polymers have received much attention because of their unique chemical structures with a large number of terminal groups which are easily functionalized according to requirements [1,2]. Therefore, many novel hyperbranched polymers have been synthesized for various applications [3–6].

Fluorinated materials are attractive recently because of their unique properties, such as extremely low energy surface, and thus excellent water and oil repellency, solvent resistance, and acid and alkali stability [7–10]. Therefore, the fluorinated materials are considered to be used for high performance coatings on different substrates, showing the good protection against corrosion, weathering, and environmental pollution [11–14].

The fluorinated hyperbranched polymers combine the advantages of both fluorinated and highly branched polymers [15–17]. The fluorinated hyperbranched polyimides were prepared and used for optical wave guide materials, showing good thermal stability and low optical absorption in the near infrared region [18]. Sangermano et al. reported that the fluorinated aromatic–aliphatic hyperbranched polyesters used as additives in cationic photopolymerization systems protected the cured coatings from aggressive solvents, enhanced the film hardness, and allowed a low energy surface [19]. In our previous work, the fluorinated hyperbranched polyester acrylates were applied into UV curing formulations, showing that the cured films possessed low surface energy and good water and oil repellence [20].

In this work, a series of hyperbranched polyesters with different numbers of fluorinated groups at the terminals, such as TAH*n*–HFBA and TAH*n*–DFHMA, and a linear fluorinated copolymer poly(*n*-BMA-co-DFHMA) for comparison were synthesized based on thioglycolic acid modified Boltorn^{TM} products (TAH*n*) and characterized by ^{1}H NMR spectroscopy. The synthesized fluorinated polymers were blended into the UV curable formulations as additives. After curing, the contact angle measurement was carried out for the films using water and 1-bromonaphthalene as test liquids. The results showed that the synthesized hyperbranched polymers enhanced the hydrophobicity and oleophobicity of the UV cured films. Moreover, the F/C ratio value of the UV cured film surface was detected by XPS analysis, and showed that the film with TAH20–DFHMA addition has the highest F/C value, indicating that TAH20–DFHMA has the most efficient aggregation effect at the film surface.

2. Results and discussion

2.1. Characterization

To evaluate the surface aggregation ability of different kinds of fluorinated chemicals in UV-curable formulations, two fluorinated

---

[*] Corresponding author. Tel.: +86 551 3606084; fax: +86 551 3606630.
E-mail address: wfshi@ustc.edu (W. Shi).

0022-1139/$ – see front matter © 2010 Elsevier B.V. All rights reserved.
doi:10.1016/j.jfluchem.2010.09.008

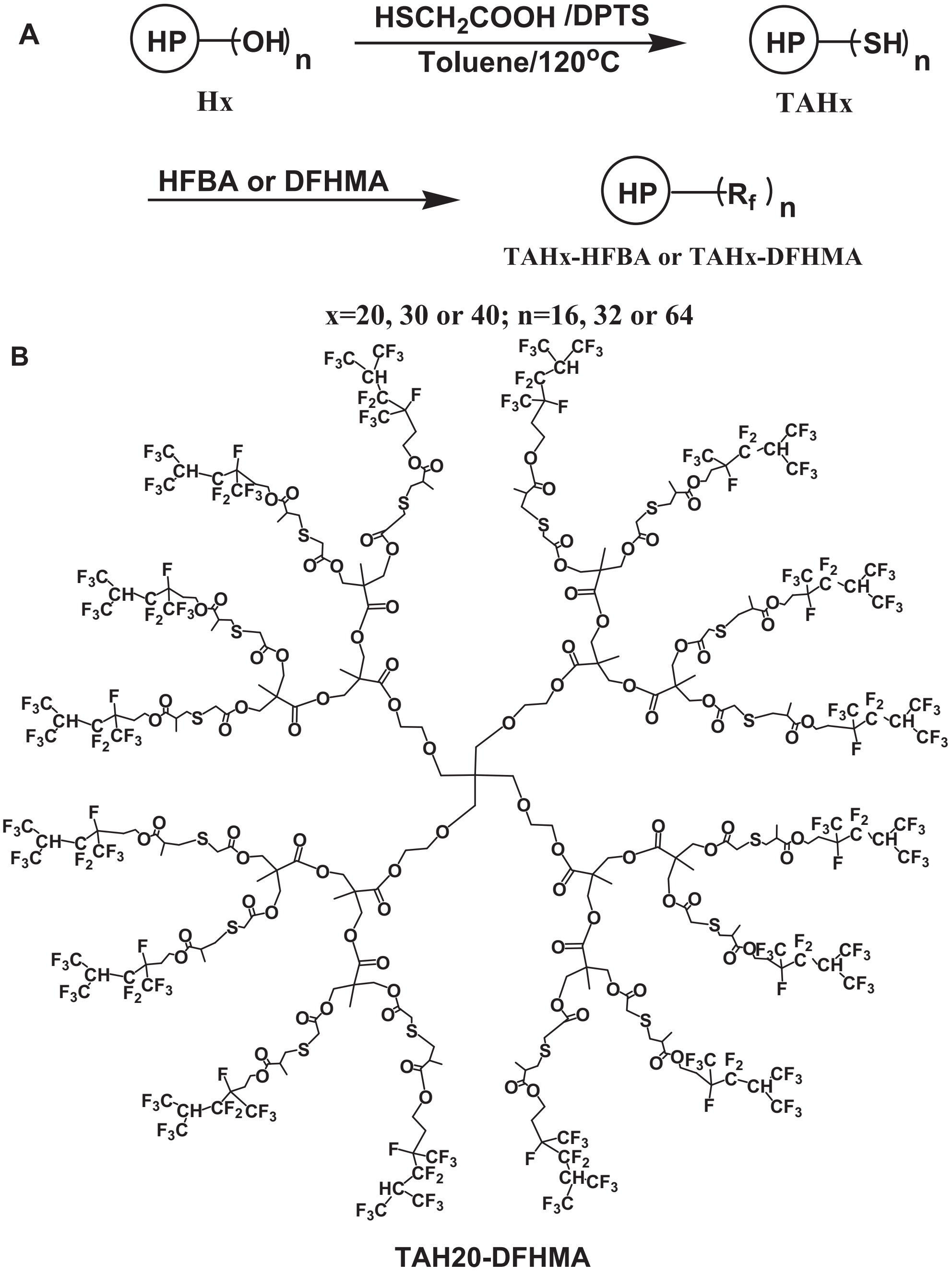

Scheme 1. Synthesis routes for fluorinated hyperbranched polymers (A) and ideal schematic representation of TAH20–DFHMA (B). (HP: Boltorn H polymer, DPTS: 4-dimethylaminopyridine p-toluenesulfonate).

monomers, hexafluorobutyl acrylate (HFBA) and dodecafluoroheptyl methacrylate (DFHMA), were used to modify the hyperbranched polyester. The synthesis route and the ideal structure of TAH20–DFHMA are shown in Scheme 1A and B, respectively. A linear copolymer, poly(*n*-BMA-co-DFHMA), was also synthesized for comparison (Scheme 2).

Boltorn^{TM} H20, H30 and H40 are a series of hyperbranched polyester and theoretically have 16, 32, and 64 terminal hydroxyl groups. The hydroxyl groups were functionalized by esterification with thioglycolic acid (TA) as shown in Scheme 1A. In the ^{1}H NMR spectrum of TAH20 in $CDCl_3$ (Fig. 1), the signals at the chemical shifts of 2.03–2.06 ppm were assigned to the thiol proton, while that at 4.29–4.39 ppm were assigned to the methylene protons of original hydroxylmethyl group in 2,2-bis(hydroxymethyl) propionate (BMPA, the structural unit of H20), which had shifted to the high δ value after esterification. According to the integration results from the NMR peaks, the thiol group number was less than the theoretically calculated value, compared with the integral value of signal peak for the methylene protons of $-CH_2-SH$ at 3.28–3.31 ppm, which was possibly because of the integral inaccuracy of active hydrogen of the thiol proton in the NMR analysis. Moreover, the signals of methylene protons of disulfides ($-CH_2-S-S-CH_2-$) at the higher chemical shifts were not observed, indicating that no apparent oxidation happened for the thiol groups. The ^{1}H NMR spectra of TAH30 and TAH40 were also shown in Fig. 1, showing the similar curves as TAH20. From the integral result, the conversion of hydroxyl group of H20 was calculated to be 98%, indicating that almost all hydroxyl groups were esterified by

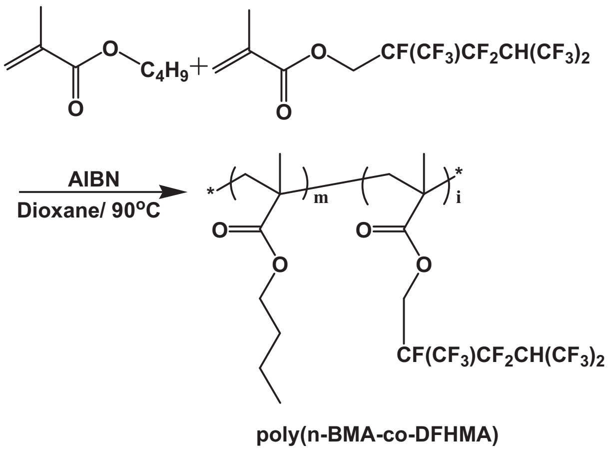

Scheme 2. Synthesis route for fluorinated linear copolymer.

thioglycolic acid. For H30 and H40, the conversion was a little lower, 95% and 92%, respectively, due to the difficult esterification of the interior hydroxyl groups resulting from the unregulated structure of H30 and H40, as well as the steric hindrance of the exterior close groups.

The fluorinated hyperbranched polymers, TAH20–HFBA, TAH20–DFHMA, TAH30–DFHMA and TAH40–DFHMA were synthesized through the thiol-ene addition reaction by hyperbranched thioglycolic acetate with fluorinated monomers. In the ^{1}H NMR spectrum of TAH20–HFBA (Fig. 2), the peaks of methine proton of –CFH– and methylene protons of $–CH_2–CF_2–$ were observed at 5.30–4.88 ppm and 4.66–4.45 ppm, respectively, which proved the presence of hexafluorobutyl groups. The two peaks at the chemical shift of 3.06–2.72 ppm were assigned to the methylene protons of $–S–CH_2–CH_2–C(O)O–$ group, and their integral values were nearly the same, from which it could be judged that the sulfur atoms were completely added onto the β-carbon atoms of hexafluorobutyl acrylate. By comparing the integral values of the peaks at the chemical shift of 3.31–3.28 (the methylene protons of $–O(O)C–CH_2–S–$) and 3.06–2.72, it could be found that over 99% thiol groups were modified.

In the ^{1}H NMR spectrum of TAH20–DFHMA, the peaks at the chemical shifts of 5.79–5.33 and 4.88–4.42 ppm were assigned to the methine proton of $–CH(CF_3)_2$ and the methylene protons of $–CH_2–CF_2–$, respectively, which indicated the presence of dodecafluoroheptyl group. The shape of peaks was more complicated than that for TAH20–HFBA, because dodecafluoroheptyl methacrylate had an isomer with fluorinated group $–CF(CF_2CF_3)CH(CF_3)_2$. The peaks at the chemical shift of 2.99–2.68 ppm were assigned to the methine and methylene protons of $–S–CH_2–CH(CH_3)–C(O)O–$ group. By comparing the integral values of the peaks at the chemical shift of 3.33–3.28 (the methylene proton of $–O(O)C–CH_2–S–$) and 2.99–2.68, it could be calculated that about 95% thiol groups were modified. Here, the thiol group conversion was a little lower than that in the reaction with HFBA, mostly because of the steric hindrance of $–CH_3$ in DFHMA.

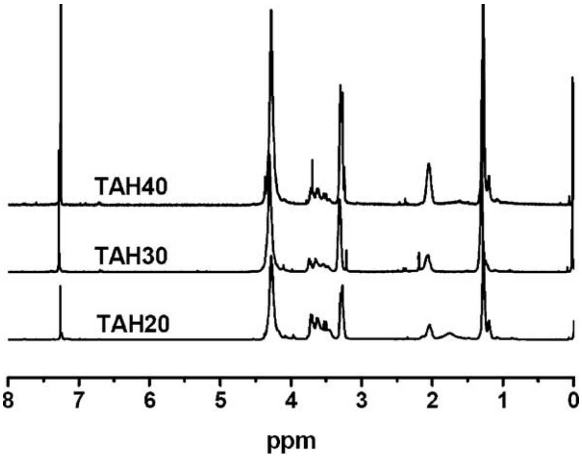

Fig. 1. ^{1}H NMR spectra of TAH20, TAH30 and TAH40.

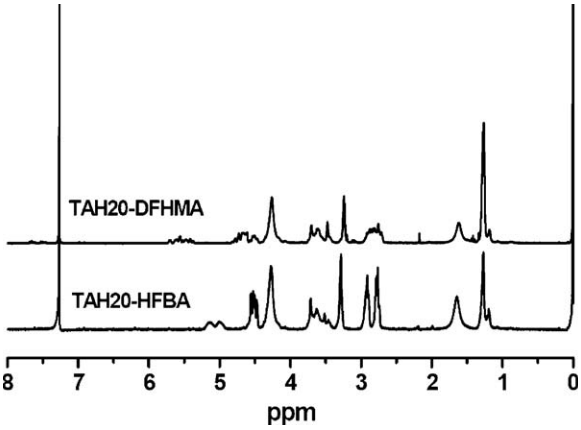

Fig. 2. ^{1}H NMR spectra of TAH20–HFBA and TAH20–DFHMA.

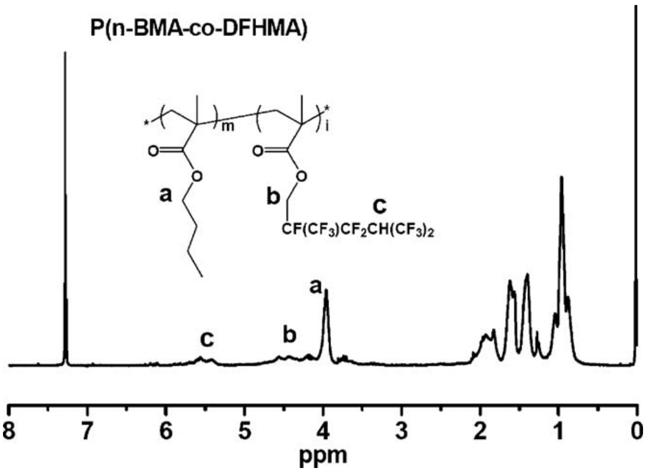

Fig. 3. ^{1}H NMR spectrum of poly(*n*-BMA-co-DFHMA).

The linear copolymer poly(*n*-BMA-co-DFHMA) was synthesized as shown in Scheme 2, and the ^{1}H NMR spectrum is shown in Fig. 3. The peak at the chemical shift of 4.12–3.82 ppm was assigned to the ethylene protons of $–OCH_2–$ in poly(*n*-BMA) chain. The peaks at the chemical shifts of 4.82–4.12 ppm and 5.79–5.33 ppm were assigned to the methylene protons of $–OCH_2–$ and methine proton of $–CH(CF_3)_2$ in poly(DFHMA) chain. According to the ratio of integral values of the peaks b (or c) and a, the constitution of the copolymer could be calculated: poly(*n*-BMA)/poly(DFHMA) = 0.62/0.38 (1.63), which was a little lower than the feed ratio because of the higher polymerization reactivity of DFHMA than BMA.

2.2. Water and oil repellency of the UV cured films

A common method to determine the wettability of a solid surface was to obtain a contact angle. A series of samples were prepared by adding the fluorinated monomers (i.e., HFBA or DFHMA) and the modified hyperbranched polyesters (i.e., TAH20, TAH30 or TAH40) or the linear copolymer (poly(*n*-BMA-co-

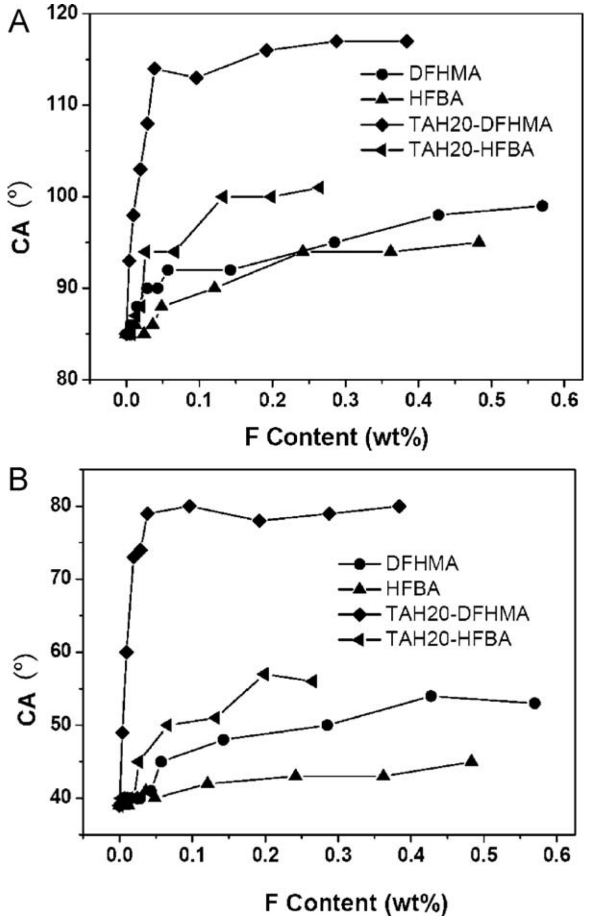

Fig. 4. Contact angle values of cured films with fluorinated monomers and their polymers: (A) water; (B) 1-bromonaphthalene.

DFHMA)) to EB270/HDDA at fluorine concentrations ranging from 0.01 wt% to about 0.6 wt%, followed by exposing to a Fusion UV lamp to obtain the cured transparent films. The contact angle measurement was carried out on the films using water and 1-bromonaphthalene as test liquids.

The water and oil contact angles of the UV cured films containing HFBA and TAH20–HFBA compared with DFHMA and TAH20–DFHMA were presented in Fig. 4A and B, respectively. Apparently, both the films containing monomers DFHMA and FHBA had little enhancement in the contact angle values for either water or 1-bromonaphthalene. However, the films added with their hyperbranched polymers, especially TAH20–DFHMA, had much higher contact angle values, reaching to 117° for water and 80° for 1-bromonaphthalene. Therefore, the fluorinated hyperbranched polymers were more efficient than the fluorinated monomers on improving the hydrophobic and oleophobic ability of UV cured film.

It was also found that the molecular structure of DFHMA-based polymers affects the water and oil repellency of the film. The fluorinated hyperbranched polymers with highly branched cores, TAH20–DFHMA, TAH30–DFHMA and TAH40–DFHMA, as well as the copolymer poly(*n*-BMA-co-DFHMA), were used for comparison, and the contact angle results of their cured films were shown in Fig. 5A and B. It can be seen that all the fluorinated polymers were effective in improving the hydrophobicity and olephobicity even at a very low fluorine content. For the hyperbranched polymers, the contact angle increased steeply at the fluorine content of below 0.1 wt%, then reached to an almost constant value as the fluorine content further increased. For the copolymer poly(*n*-BMA-co-DFHMA), the similar tendency could be observed but possessing lower contact angles at higher fluorine content of 0.2 wt%. The maximal contact angles of all the fluorinated hyperbranched polymer film reached 117° for water and 80° for 1-bromonaphthalene, which were higher than that for poly(*n*-BMA-co-DFHMA). Thus, the fluorinated hyperbranched polymers endowed the films with stronger capability of water and oil repellence than the linear poly(*n*-BMA-co-DFHMA).

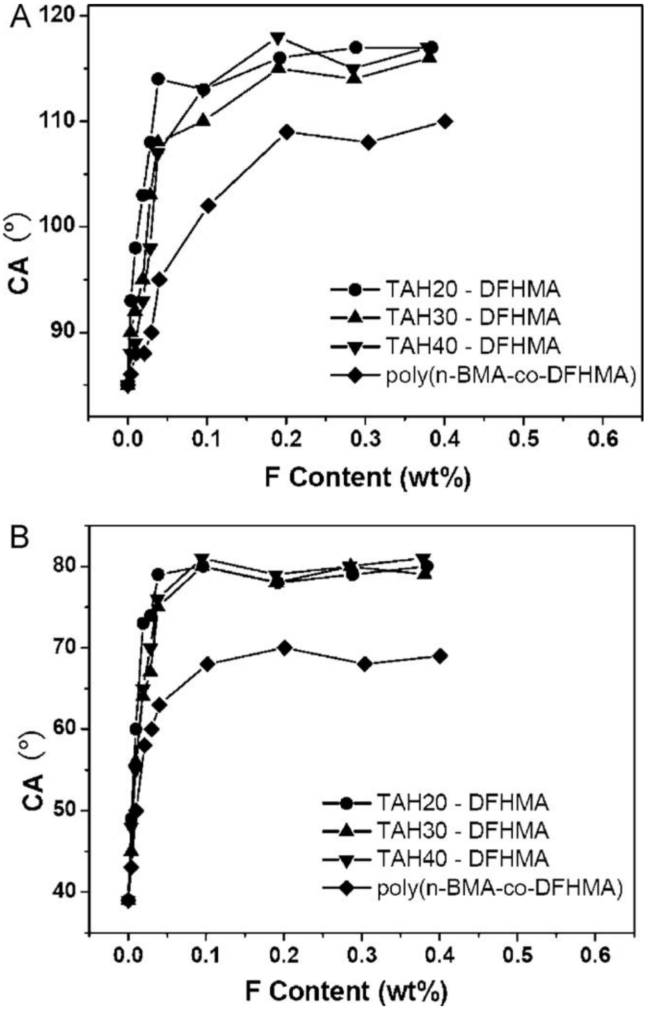

Fig. 5. Contact angle values of cured films with fluorinated polymers: (A) water; (B) 1-bromonaphthalene.

2.3. Chemical composition of the UV cured films

To understand the enhancement in hydrophobic and oleophobic ability of cured films, XPS analysis was performed to determine the element content at the film surface.

The XPS spectrum of cured film with the addition of 0.05 wt% TAH20–DFHMA was shown in Fig. 6A with the chemical composition of C1s, N1s, O1s and F1s. From the survey scan, the signals of fluorine, oxygen, nitrogen and carbon could easily be observed, with bonding energies of 688, 532, 399 and 290 eV, respectively. The high-resolution C1s XPS spectrum (Fig. 6B) showed four different binding energies. The peaks at around 283.5, 284.8, 287.8 and 292.4 eV were assigned to the binding energy of four kind carbon atoms, C–C, C–O, C(O)OH, and C–F, respectively.

The XPS analysis was also performed for the films with TAH20–DFHMA, TAH30–DFHMA, TAH40–DFHMA and poly(*n*-BMA-co-DFHMA) at three concentrations. The F/C ratios calculated from the

Table 1
F/C ratios of the cured film surface with TAH20–DFHMA, TAH30–DFHMA, TAH40–DFHMA, and poly(*n*-BMA-co-DFHMA).

F content in bulk (g/g)	F/C ratio			
	TAH20–DFHMA	TAH30–DFHMA	TAH40–DFHMA	Poly(*n*-BMA-co-DFHMA)
1.92×10^{-4}	0.36	0.28	0.27	0.24
3.84×10^{-4}	0.38	0.36	0.37	0.28
1.92×10^{-3}	0.38	0.37	0.36	0.31

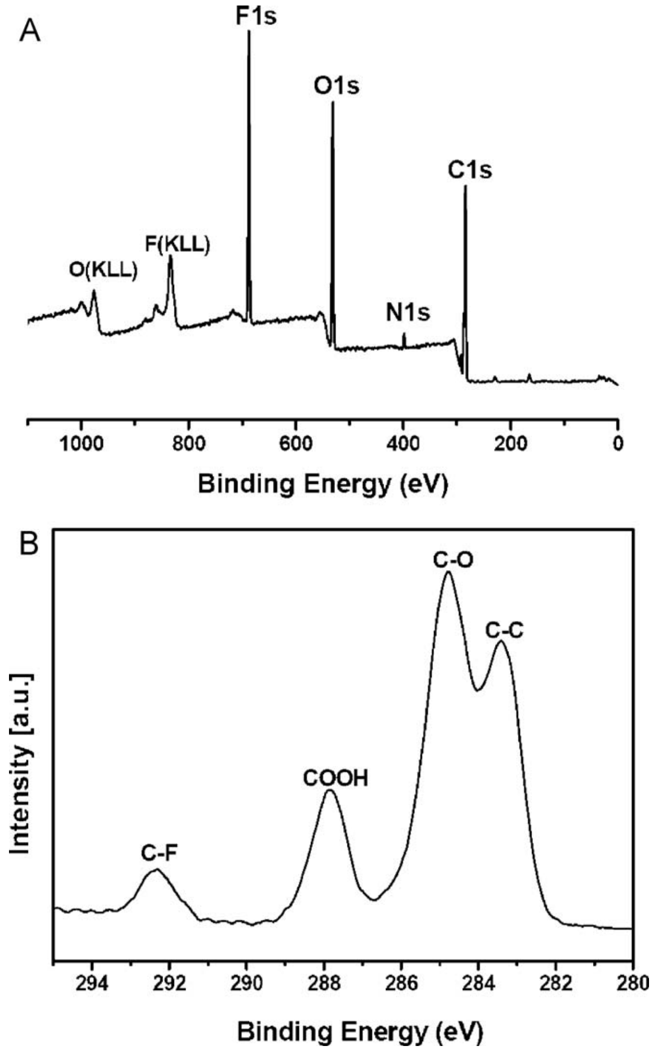

Fig. 6. XPS spectrum of UV cured film with addition of 0.05 wt% TAH20–DFHMA (A) and its high-resolution C1s spectrum (B).

XPS curves are listed in Table 1. The fluorine content in the bulk was calculated from the addition content of the fluorinated polymer and the fluorine percent of the polymer itself (calculated from the molecular structure). Obviously, F/C ratio increased with the increasing polymer content. However, F/C ratio increased little with addition of TAH20–DFHMA, whereas with addition the other three polymers, it increased evidently when the fluorine content increased from 1.92×10^{-4} to 1.92×10^{-3}. This indicated that at the low fluorine content, 1.92×10^{-4}, TAH20–DFHMA showed efficient aggregation at the cured film surface. It was possibly because TAH20–DFHMA had a smaller molecular radius and more regular space structure than the other hyperbranched polymers (H20 had more regular space structure than H30 and H40), which resulting less molecular chain entanglement and thereby making it easy to aggregate at the surface. On the other hand, the film added with poly(*n*-BMA-co-DFHMA) showed the lowest F/C ratio at three fluorine contents, which was due to the entanglement molecular chain of poly(*n*-BMA-co-DFHMA), making difficult to aggregate at the film surface. For the fluorinated monomers, the F/C ratios were found to be nearly zero at three fluorine contents, indicating the poor ability of aggregating at the film surface, resulting from their good solubility in the resins. As a result, the synthesized fluorinated hyperbranched polyesters performed perfect aggregation effect to the film surface.

3. Conclusion

The fluorinated hyperbranched polymers and linear copolymer were synthesized successfully and characterized by ^1H NMR spectroscopy. The obtained polymers were used for UV-curable formulations as additives. The wettability of the cured film surface was investigated by contact angles measurement with water and 1-bromonaphthalene. The results showed that all the polymeric additives can enhance the hydrophobicity and oleophobicity of cured films, especially DFHMA-based additives, which drastically altered the wettability of films due to the higher F/C ratio.

4. Experimental

4.1. Materials

Dodecafluoroheptyl methacrylate (DFHMA) and hexafluorobutyl acrylate (HFBA) were supplied by XEOGIA Fluorine-Silicon Chemical Co., Ltd., China. *n*-Butyl methacrylate (*n*-BMA), thioglycolic acid, 4-dimethylamino pyridine (DMAP), p-toluene sulfonic acid (PTSA), 2,2′-azobisisobutyronitrile (AIBN), toluene and tetrahydrofuran were supplied by Shanghai First Reagent Co., China. The hyperbranched aliphatic polyester Boltorn^{TM} H20, Boltorn^{TM} H30 and Boltorn^{TM} H40 (defined as H20, H30 and H40), theoretically with 16, 32, 64 of terminal hydroxyl groups, were supplied by Perstorp AB, Sweden. The photoinitiator, 2-hydroxy-2-methyl-1-phenyl-1-propanone (Runtecure 1103) was supplied by Runtec Co., China. 1,6-Hexyldiol diacrylates (HDDA) was supplied by Eternal Chemical Co., Taiwan. Polyurethane acrylate (EB270) was supplied by Cytec, USA.

4-Dimethylaminopyridine p-toluenesulfonate (DPTS) as a catalyst was prepared according to the literature [21].

4.2. Measurements

The ^1H NMR analyses were carried out on a Bruker 300 MHz nuclear magnetic resonance instrument (Bruker Bio-Spin Co., Switzerland) with $CDCl_3$ as a solvent and tetramethylsilane (TMS) as an internal reference.

The contact angle measurement was performed with a JC2000A instrument at room temperature (20 °C) with the sessile drop technique. Two films of each sample were prepared for contact angle measurement, and at least eight measurements were performed on each film. The difference from the average value was no more than 8°.

The X-ray photoelectron spectroscopy (XPS) data were obtained using a physical electronics (ESCALABMKII) XPS/ESCA system. The takeoff angle of the electron was 90° with respect to the surface of the sample.

4.3. Synthesis

4.3.1. Synthesis of hyperbranched thioglycolic acetate

H20 was modified by end-capping thioglycolic acid to obtain the hyperbranched thioglycolic acetate (TAH20) as proposed by Fu et al. [22]. Thioglycolic acid (11.05 g, 0.12 mol), H20 (10.94 g, 6.25 mmol, 0.10 mol –OH) and DPTS (0.65 g, 3.0 wt%) were dissolved in 100 mL of toluene in a three-necked round-bottomed flask, and stirred overnight at 120 °C under refluxing. Then toluene was removed under reduced pressure at room temperature. The obtained crude product was diluted with 50 mL of CH_2Cl_2, washed with saturated $NaHCO_3$ aq. (three times), saturated NaCl aq. (twice) and then distilled water, and dried with anhydrous Na_2SO4. After that, Na_2SO4 was removed by filtration and CH_2Cl_2 was evaporated under reduced pressure. The product, named TAH20, was obtained as a colorless viscous oil with a yield of 85%. ^1H NMR ($CDCl_3$) of TAH20: δ (ppm) 1.09–1.34 ($-CH_3$, 36H), 2.03–2.06 ($-SH$, 12H), 3.28–3.31 ($-CH_2-S-$, 28H), 3.47–3.73 ($-CH_2-OH$, $-CH_2-CH_2-$, 20H), 4.29–4.39 ($-CH_2-COO-$, 56H).

The hyperbranched thioglycolic acetate, TAH30 and TAH40, based on H30 and H40 were also synthesized through the same procedure by substituting H20 with H30 and H40, respectively.

TAH30: viscous oil; yield: 82%; ^1H NMR ($CDCl_3$): δ (ppm) 1.09–1.34 ($-CH_3$, 112H), 2.03–2.06 ($-SH$, 30H), 3.28–3.31 ($-CH_2-S-$, 58H), 3.47–3.73 ($-CH_2-OH$, $-CH_2-CH_2-$, 24H), 4.29–4.39 ($-CH_2-COO-$, 120H).

TAH40: viscous oil; yield: 80%; ^1H NMR ($CDCl_3$): δ (ppm) 1.09–1.34 ($-CH_3$, 180H), 2.03–2.06 ($-SH$, 48H), 3.28–3.31 ($-CH_2-S-$, 112H), 3.47–3.73 ($-CH_2-OH$, $-CH_2-CH_2-$, 28H), 4.29–4.39 ($-CH_2-COO-$, 240H).

4.3.2. Synthesis of fluorinated hyperbranched thioglycolic acetate

TAH20 (1.25 mmol, 3.31 g) and HFBA (20 mmol, 4.72 g) were dissolved in THF (40 mL) in a 100 mL-round-bottomed flask. Then triethylamine (0.08 g, 1.0 wt%) was added as a catalyst. The mixture was stirred at room temperature for 24 h. After the removal of THF and excess HFBA under reduced pressure, the product, named TAH20–HFBA, was obtained as a yellowish viscous liquid (yield: 95%). ^1H NMR ($CDCl_3$) of TAH20–HFBA: δ (ppm) 1.09–1.34 ($-CH_3$, 36H), 2.72–3.06 ($-S-CH_2-CH_2-C(O)O-$, 56H), 3.28–3.31 ($-CH_2-S-$, 28H), 3.47–3.73 ($-CH_2-OH$, $-CH_2-CH_2-$, 20H), 4.29–4.39 ($-CH_2-COO-$, 56H), 4.45–4.66 ($-C(O)O-CH_2-CF_2-$, 28H), 4.88–5.30 ($-CHF-CF_3$, 14H).

TAH20–DFHMA was produced in the same process by substituting HFBA with DFHMA. It was obtained as a yellow viscous liquid (yield: 90%). ^1H NMR ($CDCl_3$) of TAH20–DFHMA: δ (ppm) 1.09–1.43 ($-CH_3$, 36H), 2.68–2.99 ($-S-CH_2-CH(CH_3)-C(O)O-$, 56H), 3.28–3.33 ($-CH_2-S-$, 28H), 3.47–3.74 ($-CH_2-OH$, $-CH_2-CH_2-$, 20H), 4.29–4.39 ($-CH_2-COO-$, 56H), 4.42–4.88 ($-C(O)O-CH_2-CF-$, 28H), 5.33–5.79 ($-CH(CF_3)_2-$, 14H).

According to the same procedure, the molar ratios of 1:32 and 1:64 for TAH30 and TAH40 to DFHMA, respectively, were used to prepare TAH30–DFHMA (yield: 88%) and TAH40–DFHMA (yield: 85%).

4.3.3. Synthesis of P(n-BMA-co-DFHMA)

n-BMA (20 mmol, 2.84 g), DFHMA (10 mmol, 4.00 g) and AIBN (0.8 mmol, 0.13 g) were dissolved in dioxane (50 mL) in a 100 mL-round-bottomed flask, and stirred at 90 °C for 12 h. After dioxane was removed under reduced pressure, the product, named poly(*n*-BMA-co-DFHMA), was obtained as an colorless viscous liquid (yield: 95%). ^1H NMR ($CDCl_3$) of P(*n*-BMA-co-DFHMA): δ (ppm) 0.73–1.18 ($-CH_3$, 40H), 1.20–2.21 ($-CH_2-$, 36H), 3.82–4.12 ($-O-CH_2-CH_2-$, 10H), 4.12–4.82 ($-O-CH_2-CF-$, 6H) 5.33–5.79 ($-CH(CF_3)_2-$, 3H).

4.3.4. Sample preparation

HFBA, DFHMA, TAH20–FHBA, TAH20–DFHMA, TAH30–DFMHMA, TAH40–DFHMA, and poly(*n*-BMA-co-DFHMA) together with 3 wt% Runtecure 1103 were added as additives into the resin EB270/HDDA with a weight ratio of 7:3 in different weight percentages, respectively, and stirred vigorously until the homogenous solution formed. The mixture then exposed to a medium pressure mercury lamp (2 kW, Fusion system, USA) to obtain the UV-cured films used for the contact angle and XPS measurements.

Acknowledgment

The financial support of National Natural Science Foundation of China (No. 50633010) is gratefully acknowledged.

References

[1] S. Peleshanko, R. Gunawidjaja, S. Petrash, V.V. Tsukruk, Macromolecules 39 (2006) 4756–4766.
[2] I.A. Gorodetskaya, A.A. Gorodetsky, E.V. Vinogradova, R.H. Grubbs, Macromolecules 42 (2009) 2895–2898.
[3] J.H. Lee, K.S. Lee, Mol. Cryst. Liq. Cryst. 371 (2001) 341–344.
[4] J. Li, Z. Bo, Macromolecules 37 (2004) 2013–2015.
[5] H. Liang, D. Yu, Y. Xie, C. Min, J. Zhang, G. Hu, Polym. Eng. Sci. 49 (2009) 2189–2194.
[6] T.V. Richter, F. Schüler, R. Thomann, R. Mülhaupt, S. Ludwigs, Macromol. Rapid Commun. 30 (2009) 579–583.
[7] K. Wood, Macromol. Symp. 187 (2002) 469–479.
[8] M. Berglin, K.J. Wynne, P. Gatenholma, J. Colloid Interface Sci. 257 (2003) 383–391.
[9] Z. Li, Y. Xing, J. Dai, Appl. Surf. Sci. 254 (2008) 2131–2135.
[10] C. Aulin, A. Shchukarev, J. Lindqvist, E. Malmströma, L. Wågberg, T. Lindströmd, J. Colloid Interface Sci. 317 (2008) 556–567.
[11] A. Shi, S. Koka, J. Ullett, Prog. Org. Coat. 52 (2005) 196–209.
[12] N.D. Tran, N.K. Dutta, N.R. Choudhury, Polym. Degrad. Stabil. 91 (2006) 1052–1063.
[13] A. Torrisi, N. Tuccitto, G. Maccarrone, A. Licciardello, Appl. Surf. Sci. 255 (2008) 1527–1530.
[14] H. Wang, J. Fang, T. Cheng, J. Ding, L. Qu, L. Dai, X. Wang, T. Lin, Chem. Commun. 7 (2008) 877–879.
[15] C. Pitois, R. Vestberg, M. Rodlert, E. Malmström, A. Hult, M. Lindgren, Opt. Mater. 21 (2002) 499–506.
[16] W. Du, A.M. Nyström, L. Zhang, K.T. Powell, Y. Li, C. Cheng, S.A. Wickline, K.L. Wooley, Biomacromolecules 9 (2008) 2826–2833.
[17] H. Gao, D. Wang, W. Jiang, S. Guan, Z. Jiang, J. Appl. Polym. Sci. 109 (2008) 2341–2346.
[18] J.K. Park, D.H. Song, B.J. Lee, B.J. Song, J.B. Oh, H.K. Kim, J. Polym. Sci. Part A: Polym. Chem. 44 (2006) 1326–1342.
[19] M. Sangermano, A. Di Gianni, R. Bongiovanni, A. Priola, B. Voit, D. Pospiech, D. Appelhans, Macromol. Mater. Eng. 290 (2005) 721–725.
[20] H. Miao, L. Cheng, W. Shi, Prog. Org. Coat. 65 (2009) 71–76.
[21] J.S. Moore, S.I. Stupp, Macromolecules 23 (1990) 65–70.
[22] Q. Fu, J. Liu, W. Shi, Prog. Org. Coat. 63 (2008) 100–109.